The American Journal of Pathology, Vol. 177, No. 1, July 2010

DOI: 10.2353/ajpath.2010.100007

Biophysical Imaging and Computational Biology

Novel Molecular Imaging Approach for Subclinical Detection of Iritis and Evaluation of Therapeutic Success

Fang Xie,*†‡ Dawei Sun,*‡§ Alexander Schering,*‡ Shintaro Nakao,*‡ Souska Zandi,*‡ Ping Liu,† and Ali Hafezi-Moghadam*‡

From the Department of Ophthalmology, and the Massachusetts Eye & Ear Infirmary,‡ Harvard Medical School, Boston, Massachusetts; the Department of Ophthalmology,† the 1st Affiliated Hospital of Harbin Medical University, Harbin, China; and the 2nd Affiliated Hospital of Harbin Medical University,§ Harbin, China*

There is an urgent need for early diagnosis in medicine, whereupon effective treatments could prevent irreversible tissue damage. Acute anterior chamber inflammation is the most common form of uveitis and a major cause of vision loss. The proximity of the iris vasculature to the light-permeable cornea and its involvement in ocular inflammation make it an ideal target for noninvasive molecular imaging. To accomplish this, carboxylated fluorescent microspheres (MSs) were conjugated with recombinant P-selectin glycoprotein ligand-1 and systemically injected in endotoxin-induced uveitic animals. MS adhesion in the microcirculation of the anterior and posterior chamber was visualized by intravital microscopy and scanning laser ophthalmoscopy. In iritic animals, significantly higher numbers of recombinant P-selectin glycoprotein ligand-1-conjugated MSs adhered to the endothelium ($P = 0.03$) matching the increase in leukocyte adhesion. Conjugated MSs specifically interacted with firmly adhering leukocytes, allowing quantification of the endogenous immune response. Topical eye drop treatment with dexamethasone ($P < 0.01$) or cyclosporine A ($P < 0.01$) significantly lowered MS adhesion in iris vessels. Surprisingly, topical dexamethasone significantly reduced MS interaction in the fundus vessels ($P < 0.01$), while cyclosporine A did not. *In vivo* MS accumulation preceded clinical signs of anterior uveitis and leukocyte adhesion in iris vasculature. This work introduces noninvasive subclinical detection of endothelial injury in the iris vasculature, providing a unique opportunity for quantifying vascular injury and immune response *in vivo*. *(Am J Pathol 2010, 177:39–48; DOI: 10.2353/ajpath.2010.100007)*

Uveitis is the most common form of inflammatory eye disease and a major cause of vision loss.[1] Uveitis can affect any part of the eye, including the choroid and iris, and is characterized by the accumulation of leukocytes in ocular tissues.[2] Acute anterior uveitis is the most common form of uveitis. Early detection of ocular vascular injury would help to establish the diagnosis, whereupon effective treatments such as corticosteroids could halt inflammation before irreversible structural damages occur.

Clinically, iritis presents itself with nonspecific signs, such as blurred vision, conjunctival congestion, or ophthalmalgia. Complications of iritis include cataract and secondary glaucoma. Precise evaluation of the iris vasculature in fluorescein angiography is complicated by its pigmentation and the considerable amount of constitutive leakage under normal conditions. Iris indocyanine green angiography visualizes details of the vascular pattern in the iris, providing a useful means to study its structure and hemodynamics in normal and newly formed iris vessels.[3] However, these existing techniques detect disease at an established stage, when structural damage is either present or inevitable. Techniques that would allow evaluation of leukocyte-endothelial interaction in the iris or choriocapillaris flow or identification of specific molecular changes in patients are not available.

Supported by NIH grants AI050775 (A.H.-M.), American Health Assistance Foundation (A.H.-M.), a Science & Technology project of Heilongjiang Province, China (GB06C40104 to D.S.), and the Malaysian Palm Oil Board (A.H.-M.).

F.X. and D.S. contributed equally to this work.

Accepted for publication March 24, 2010.

rPSGL-Ig was a gift from Y's Therapeutics (Bruno, CA).

Supplemental material for this article can be found on *http://ajp.amjpathol.org*.

Address reprint requests to Ali Hafezi-Moghadam, M.D., Ph.D., Angiogenesis Laboratory, 325 Cambridge St., 3rd Floor, Boston, MA 02114. E-mail: ali_hafezi-moghadam@meei.harvard.edu.

An established model of acute ocular inflammation is the endotoxin-induced uveitis (EIU), caused by systemic lipopolysaccharide (LPS) injection.[4] In this model both posterior and anterior chambers (AC) show a pronounced inflammatory response, allowing quantitative comparison of the time course and extent of vascular injury in the iris with the vasculitis in the posterior chamber. Intravital imaging of the AC inflammation has provided invaluable insights into ocular immunology.[5–8]

Recently, we introduced a novel imaging technique for detection of endothelial surface molecules in acute ocular inflammation.[9,10] Our approach is founded on certain aspects of leukocyte-endothelial interaction, a common component in the pathogenesis of various ocular diseases. Leukocytes normally do not interact with the endothelium of blood vessels, save for occasional tethering. However, at sites of inflammation, endothelial cells express adhesion molecules, such as P-selectin that facilitate the multistep leukocyte recruitment cascade.[11] The steps of the recruitment process include tethering, rolling, firm adhesion, and transmigration into the extravascular space.[12,13] The main selectin ligand, P-selectin glycoprotein ligand-1 (PSGL-1), is a 240-kd disulfide-bonded homodimeric mucin-like glycoprotein, which is expressed on myeloid cells and a subset of lymphocytes.[14] PSGL-1 binds to all three selectins, P-, E-, and L-selectin, and mediates leukocyte interaction with endothelial cells, platelets, and other leukocytes.[15,16] Under flow conditions, PSGL-1 interaction with P-selectin on the surface of activated endothelium mediates tethering and rolling.[17,18] By designing adhesion molecule-conjugated fluorescent microspheres (MSs) that target specific endothelial surface molecules in combination with noninvasive imaging we showed early endothelial injury in ocular microvessels of live animals.[9,10,13]

In this work, we use our new molecular imaging approach to detect earliest signs of iritis *in vivo* and correlate the injury in the AC with that in the retinal and choroidal vasculature. Furthermore, we use our adhesion molecule-conjugated imaging agents to quantify and follow up on the treatment success of current anti-iritis agents.

Materials and Methods

Endotoxin-Induced Uveitis

All experiments were performed in accordance with the ARVO Statement for the Use of Animals in Ophthalmic and Vision Research and were approved by the Animal Care and Use Committee of the Massachusetts Eye & Ear Infirmary. Male Lewis rats (8–10 weeks old) were obtained from Charles River (Wilmington, MA). Iritis was induced in rats by injecting 100 μg of LPS (*Salmonella typhimurium*; Sigma Chemical, St. Louis, MO) diluted in 100 μl of sterile saline into one hind footpad of each animal.[4] Control animals received a footpad injection of vehicle (saline). Animals were maintained in an air-conditioned room with a 12-hour light-dark cycle and were given free access to water and food until used in the experiments.

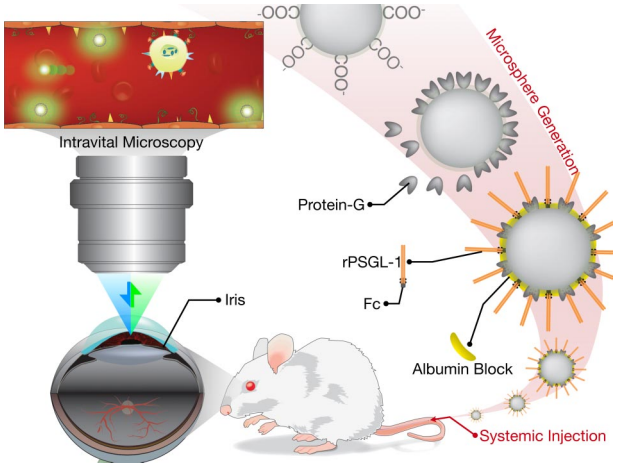

Figure 1. Schematic of the *in vivo* molecular imaging approach to quantitate endothelial injury in the iridal microcirculation. Carboxylated fluorescent microspheres are conjugated with protein G, using a carbodiimide reaction and subsequently coated with "FC" coupled rPSGL-1. To reduce nonspecific interaction, the free regions are blocked with albumin. The rPSGL-1-conjugated microspheres are then injected systemically in live animals. The iridal microcirculation is then imaged in live animals using epifluorescence intravital microscopy.

Treatments

To reduce inflammation, animals were topically treated with dexamethasone (Dex, ophthalmic suspension 0.1%, 5 ml; American Alcon Laboratories, Inc. Fort Worth, TX) or cyclosporine A eye drops (CsA, ophthalmic suspension 0.1%, 10 ml; American MEEI, Boston, MA), six times within 24 hours.

MS Preparation

Yellow-green carboxylated fluorescent MSs (2 μm, Polysciences, Inc., Warrington, PA) were covalently conjugated to protein G (Sigma), using a carbodiimide-coupling kit (Polysciences, Inc.).[13] MSs were incubated with nonimmune mouse IgG (mIgG, Southern Biotech, Birmingham, AL, catalog no. 0102-14), or recombinant P-selectin glycoprotein ligand-1 (rPSGL-1, Y's Therapeutics, Burlingame, CA) for 2 hours at room temperature on a rotary shaker and subsequently washed with PBS and bovine serum albumin (0.1%). Subsequently, MSs were washed again in PBS and sonicated before use *in vivo*. 3×10^8 MSs were injected in each animal (Figure 1).

Quantification of the rPSGL-1 on the MS Surface

The average number of rPSGL-1 molecules on the MS surfaces was determined using flow cytometry, as described previously.[13] Briefly, nonfluorescent MSs (10^6/ml, Polysciences, Inc.) conjugated to rPSGL-Ig (Y's Therapeutics) were incubated with fluorescein isothiocyanate (FITC)-conjugated mouse anti-human rPSGL-1 (KPL-1) or its isotype-matched control (BD Biosciences, Franklin Lakes, NJ) for 30 minutes, centrifuged at 4000 $\times$ *g* for 5 minutes, washed twice, and resuspended into PBS. The fluorescence intensity of 10^4 MSs was measured on a FACScan (Coulter EPICS XL), equipped with the System

Work II software. The surface expression was presented as the mean channel fluorescence on a logarithmic scale.

In parallel, calibration beads (Quantum Simply Cellular, Bangs Laboratories, Fishers, IN) were coated with reference fluorescence antibodies, as described previously.[13] Four different populations of MSs with known densities of binding sites for Fc were coated with goat anti-mouse IgG. Uncoated MSs were used as a control. A calibration curve was constructed based on the mean fluorescence intensity of the MSs.

In Vivo *Evaluation of MS Adhesion in the Iridal, Retinal, and Choroidal Vessels*

Rats were anesthetized with xylazine hydrochloride (10 mg/kg) and ketamine hydrochloride (50 mg/kg). To evaluate MS adhesion in the iridal vessel in normal and EIU animals, a 3-CCD color digital video camera (HDR-HC9; Sony, Japan), combined with a stereo microscope (Leica; Germany) was used to record continuous high-resolution iridal images. An argon blue filtering light was used as the excitation light.

To evaluate MSs in the choriocapillaris, a scanning laser ophthalmoscope (SLO; HRA2; Heidelberg Engineering, Dossenheim, Germany) was used to make continuous high-resolution fundus images, with a regular emission filter for fluorescein angiography, as the excitation (441 nm) and emission (486 nm) maxima of the MSs are comparable with that of sodium fluorescein. MSs were injected 24 hours after LPS treatment and images were recorded 30 minutes after MS injection.

Upon completion of the fundus imaging, pupils were constricted with topical 4% pilocarpine hydrochloride ophthalmic solution (15 ml, Falcon, Ltd. Fort Worth, TX). Animals were placed on the platform of the anatomy stereomicroscope, allowing flexible positioning of the animals in relation to the lens. Conjugated MSs (3×10^8/ml in saline) were continuously injected into the tail vein within 1 minute through a 30-gauge 0.5-inch needle. Thirty minutes after the initial injection of the conjugated MSs, the number of free-flowing MSs in the iridal vessels of normal and EIU rats was substantially diminished, presumably due to the interaction of the MSs with the endothelium of the vessels throughout the body. This allowed us to conveniently identify and quantify accumulated MSs in the iridal vessels as distinct stationary fluorescent marks with high contrast against the nonfluorescent background.

In Vivo *Quantification of the Interacting Imaging Agents*

The number of adherent MSs was obtained from 1-minute sections of video recordings. Live images (720p, 29.97 frames/s) were captured using QuickTime 7 Pro software (Apple Inc., Cupertino, CA) and stored as .mov container using the Apple Intermediate Codec. The files were then imported into ImageJ 1.41o (Java 1.60_15).[19] To subtract free-flowing MSs as well as reduce noise, up to 80 consecutive frames were averaged using ImageJ's *z*-stack processing option. The outcome was then converted from RGB to 8-bit and a threshold was set to reveal the high-intensity fluorescent particles. To distinguish particles that are close to each other as individual entities, images were processed using ImageJ's Watershed function. Quantification of the number of MSs was achieved using the Analyze Particle function.

Ex Vivo *Evaluation of Accumulated MSs and Leukocytes*

To prepare iridal, retinal and choroidal flat mounts, animals were anesthetized 24 hours after LPS or vehicle injection. Subsequently, 1 ml of MSs (3×10^8/ml in PBS) was injected continuously through the tail vein over 1 minute. Thirty minutes after MS injection, animals were perfused with PBS (pH 7.4) and rhodamine-labeled concanavalin-A lectin (RL-1002, Con-A; Vector Laboratories, Burlingame, CA), 10 μg/ml in PBS (pH 7.4), to stain vascular endothelial cells and firmly adhering leukocytes. To perfuse the animals, the chest cavity was opened, and a 24-gauge needle was introduced into the aorta. Drainage was achieved by opening the right atrium. PBS (50 ml) was injected to wash out intravascular content, including unbound MSs and leukocytes. This was followed by perfusion of 0.3 ml of ConA in 30 ml of PBS to stain the vascular endothelium and firmly adhering leukocytes. Subsequently, 15 ml of PBS was injected to wash out excess ConA. Immediately after perfusion, the eyeball was enucleated and microdissected. Iris, retina and choroids were flat-mounted, using a fluorescence anti-fading medium (Vectashield, Vector Laboratories). The separated iris, retina and choroids were then observed under an epifluorescence microscope (DM RXA; Leica, Deerfield, IL), with both a FITC (excitation, 488 nm; detection, 505–530 nm) and a rhodamine filter (excitation, 543 nm; detection, >560 nm). Images were obtained using a high-sensitivity digital camera, connected to a computer-assisted image analysis

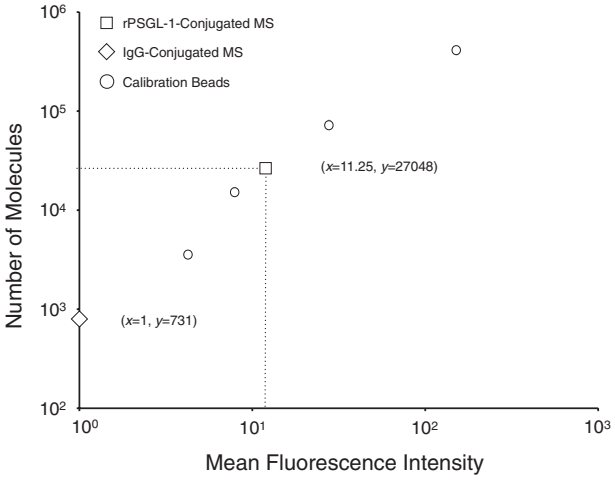

Figure 2. Quantitative analysis of the number of rPSGL-1 molecules on microspheres. Flow cytometric quantification of mean fluorescence values of calibration beads (open circles) after incubation with FITC-conjugated IgG. Mean fluorescence value of rPSGL-1-conjugated MSs (open squares) and isotype-matched control MSs (open diamonds). Calculated copy number of FITC-KPL-1 bound to rPSGL-1-conjugated or isotype control MSs, based on linear regression ($y = 2567x - 1836$, $R^2 = 0.998$).

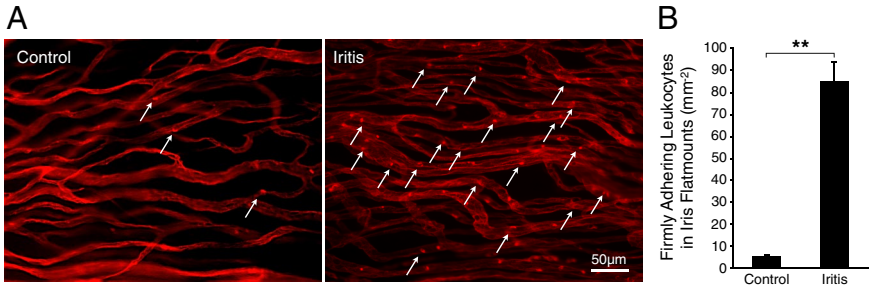

Figure 3. Conjugated MSs detect firmly adhering leukocytes. Twenty-four hours after LPS treatment, Lewis rats were perfused with PBS and rhodamine ConA to stain the vasculature and adherent leukocytes. Iris flat mounts of EIU animals were prepared. **A:** *Ex vivo* visualization of firmly adhering leukocytes in the iris microvasculature of normal and iritic animal. **Arrows** delineate firmly adhering leukocytes (bright red spots) inside the iridal microvessels. **B:** The number of firmly adhering leukocytes in iridal microvasculature per iris surface area (mm^{-2}) in control and EIU animals. $^{**}P < 0.01$.

system. Using the Openlab image analysis software (Improvision, Boston, MA), merged images of the MSs (green) with the vessel tissues (red) were generated. The number of firmly adhering leukocytes and MSs in iridal, retinal, and choroidal vessels in whole tissues was obtained by counting. In the retinal and iris flat mounts, the numbers of firmly adhering MSs were counted in the entire preparations by mosaic viewing the entire surfaces of the flat mounts under the microscope. In choroidal flat mounts, five different fields of view (optic disk, nasal, temporal, superior, and inferior) were photographed and the number of the MSs in these regions were counted, averaged, and expressed as counts per surface area (mm^{-2}), using a calibration piece under the microscope at different magnifications. MSs that interacted with leukocytes rather than vascular endothelium were distinguished and the percentage of the MSs bound to leukocytes was calculated.

Clinical Grading of Anterior Uveitis

At different time points after uveitis induction, slit-lamp examinations of the AC were performed on anesthetized animals. The scoring evaluated the absence (0) or presence (1) of flare, miosis, and hypopyon (accumulation of leukocytic exudates), in addition to the absence (0), mild presence (1), or severe presence (2) of iris hyperemia and cells in the AC. Leukocytes in the aqueous humor of the AC are visible due to their back-scattering of the incoming light. Elevated protein content of the aqueous humor causes the Tyndall effect, commonly referred to as flare. Grading of the flare is based on the ability to visualize iris and lens details. The individual results were evaluated on a cumulative scale of 0 (normal) to 7 (most severe condition).[2,20]

Statistical Analysis

All values are expressed as mean ± SEM. Data were analyzed by Student's *t*-test. Differences between the experimental groups were considered statistically significant or highly significant when the probability value, *P,* was <0.05 or <0.01, respectively.

Results

Quantification of the Number of rPSGL-1-Molecules on MSs

To quantify the number of rPSGL-1 molecules conjugated to the surface of our MSs, we covalently conjugated nonfluorescent carboxylated MSs with protein G and subsequently coated them with rPSGL-1, based on our previous report.[13] MSs were then stained with a FITC-conjugated anti-PSGL-1 mAb or isotype-matched control and their fluorescent intensities were measured by flow cytometry. The fluorescence intensity of calibration microbeads with known site densities of FITC-conjugated IgG was measured under the same flow cytometric settings. A calibration curve was generated (R^2 = 0.99892), based on which the average number of rPSGL-1 molecules (27048) on the MS surface was determined (Figure 2).

Visualization of Accumulated Leukocytes

To quantify the inflammatory response in the iris, we calculated the number of firmly adhering leukocytes per surface area of the iris. The number of firmly adhering

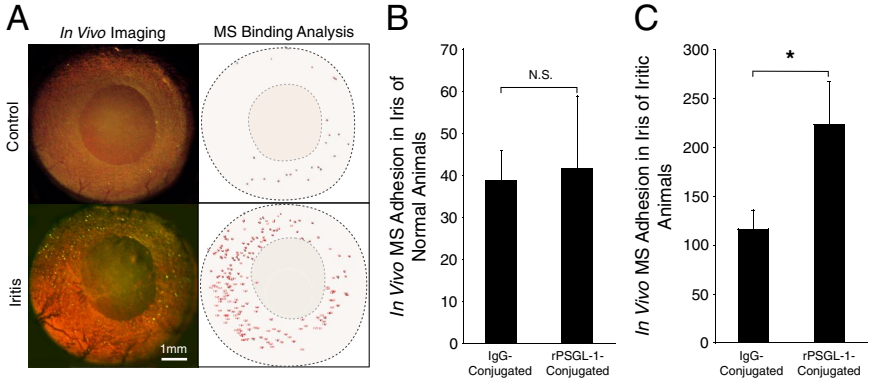

Figure 4. Noninvasive *in vivo* imaging of MS adhesion in iridal microvasculature. Anesthetized normal and iritic rats were systemically injected with rPSGL-1-conjugated fluorescent MSs, the interaction of which in the iris vasculature was visualized by intravital microscopy. **A:** Video micrographs of rPSGL-1-conjugated MS accumulation *in vivo,* 30 minutes after injection. In the video still images (**left**), yellow-green spots delineate adhering MSs. In the Image J pictures (**right**), each dot indicates one automatically counted adhering MS in the iris vessels of normal and iritic animals. **B:** Quantification of the *in vivo* accumulation of IgG- and rPSGL-1-conjugated MSs in the iris vasculature of normal animals. N.S., not significant. **C:** Quantification of the *in vivo* MS accumulation IgG- and rPSGL-1-conjugated MSs in iris vessels of uveitic animals. $^{*}P < 0.01$.

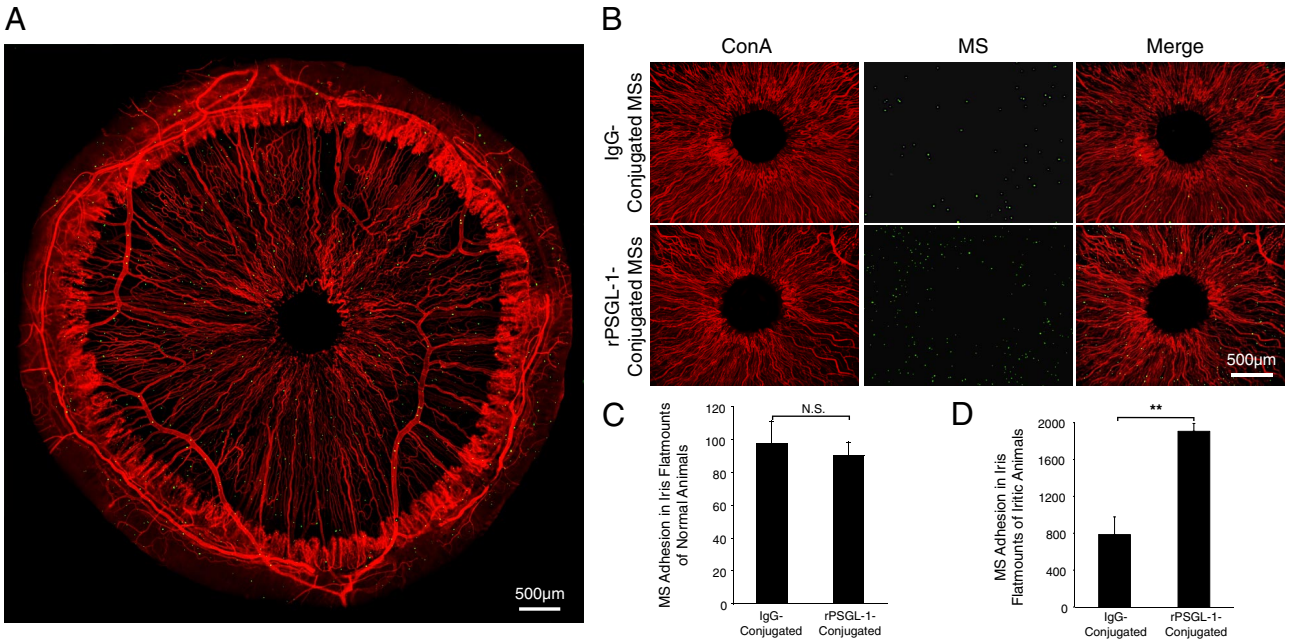

Figure 5. *Ex vivo* visualization of firmly adhering MSs in iridal vessels. 30 minutes after conjugated MSs were injected, rats were perfused with PBS and rhodamine ConA (red) to stain the iris vasculature and remove the intravascular content and nonadherent MSs. Subsequently, the iris was microsurgically excised and flat-mounted. MSs, yellow-green. **A:** Micrograph depicts *ex vivo* visualization of a whole iris flat mount from an iritis animal, injected with rPSGL-1-conjugated MSs. **B:** Micrographs depict *ex vivo* visualization of iris flat mounts from uveitic animals that were injected with IgG- or rPSGL-1-conjugated MSs. **C:** Quantification of the firmly adhering MSs in iris flat mounts of normal animals. N.S., not significant. **D:** Quantification of the firmly adhering MSs in iridal flat mounts of iritis animals. $^{**}P < 0.01$.

leukocytes in the iritic animals (84.9 ± 8.9, $n = 8$) was significantly higher than in the normal controls (5.4 ± 1, $n = 8$, $P = 3 \times 10^{-8}$) (Figure 3, A and B).

In Vivo *Accumulation of Adhesion Molecule-Conjugated MSs in Iridal Vessels*

To detect vascular injury in the iris of living animals, we investigated endothelial P-selectin expression using our rPSGL-1- or mIgG-conjugated imaging agents in normal and iritis animals. In normal animals, 30 minutes after MS injection, a low number of control (38.8 ± 7.1, $n = 5$) or rPSGL-1-conjugated (41.6 ± 17.1, $n = 5$; $P = 0.9$) MSs interacted with the endothelium of the iris vessels. In the LPS-treated animals, significantly higher numbers of rPSGL-1-conjugated MSs (223.3 ± 44.5) bound to the endothelium than IgG-conjugated controls (116 ± 19.8; $P = 0.03$) (Figure 4, A–C, and Supplemental Movie at *http://ajp.amjpathol.org*), indicating that the binding of the imaging agents parallels the physiologically relevant process of leukocyte recruitment.

Ex Vivo *Visualization of Accumulated MSs*

To examine, whether the conjugated MSs that were detected *in vivo* indeed adhered in the iridal vessels, as was judged based on the depth of focus of the fluorescent video images, we examined the MS accumulation in per-

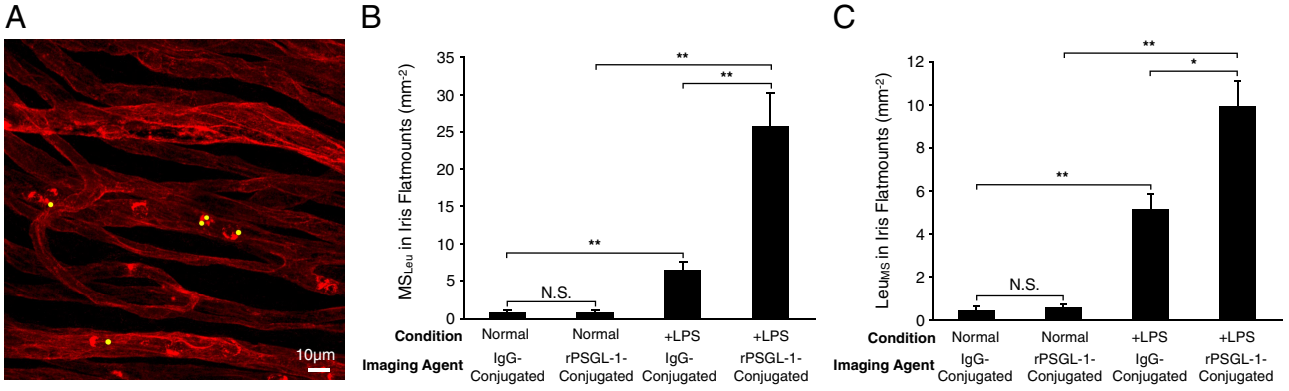

Figure 6. *Ex vivo* visualization of interaction of MSs and Leukocytes in iridal vessels. Twenty-four hours after LPS, MSs were injected, and 30 minutes later animals were perfused with PBS and rhodamine ConA (red) to stain the iris vasculature and adherent leukocytes. Iris was microsurgically excised and flat-mounted. MSs, yellow-green. **A:** Confocal micrograph of rPSGL-1-conjugated MSs in the iris microvasculature of an iritic animal. **B:** The number of IgG- or rPSGL-1-conjugated MSs adhering to leukocytes (MS_{Leu}) in iridal microvessels (mm^{-2}), in control and EIU animals. $^{**}P < 0.01$, N.S., not significant. **C:** The number of leukocytes binding to MSs (Leu_{MS}) in iridal microvessels (mm^{-2}) in control and EIU animals, injected with IgG- or PSGL-1-conjugated MSs. $^{*}P < 0.05$; $^{**}P < 0.01$; N.S., not significant.

fused *ex vivo* tissue preparations (flat mounts). Epifluorescence microscopy of the iris flat mounts showed specific adhesion of the MSs in the iridal vessels (Figure 5, A and B). In line with our *in vivo* fluorescence video microscopy, the number of the mIgG-conjugated-MSs in the iris flat mounts (90.2 ± 8.3, $n = 6$) did not significantly differ from rPSGL-1-conjugated MSs (97.6 ± 13.5, $n = 8$, $P = 0.6$). The adhesion number of rPSGL-1-conjugated MSs to the iridal vessels of iritic animals (1905.7 ± 85.4, $n = 8$) was significantly higher than mIgG-conjugated controls (785.8 ± 143.7, $n = 5$, $P = 0.0003$) (Figure 5, C and D).

MS Localization

To investigate whether the MSs are within the vessels, we used fluorescent confocal microscopy. The three-dimensional reconstruction of our iridal flat mounts showed that all MSs were indeed inside the vessels. These studies further confirmed that some of the accumulated MSs directly bound to the vascular endothelium, while others bound to firmly adhering leukocytes (Figure 6A and Supplemental Movie at *http://ajp.amjpathol.org*).

Conjugated MSs Detect Firmly Adhering Leukocytes

To examine, whether adhesion-molecule-conjugated MSs detect firmly adhering leukocytes, we calculated the number of MSs bound to firmly adhering leukocytes (MS_{Leu}) in the iridal vessels per total iridal surface. In iritis animals the numbers of rPSGL-1-conjugated MSs were significantly higher than MS_{Leu} (25.7 ± 4.6, $n = 8$) compared with the mIgG-conjugated group (6.4 ± 1.2, $n = 5$, $P = 0.03$). Furthermore, rPSGL-1-conjugated MSs showed significantly higher MS_{Leu} in the iritic animals, compared with normal controls (0.8 ± 0.3, $n = 8$, $P = 0.0008$) (Figure 6B).

Visualization of Accumulated Leukocytes Using Conjugated MS

To evaluate the interactivity of the adherent leukocytes with the conjugated MSs, we obtained the number of firmly adhering leukocytes bound to or incorporating MSs (Leu_{MS}) in the vessels of the entire iris. In the perfused iris flat mounts, a substantial number of leukocytes adhered to the iridal vessels, and many of the firmly adhering leukocytes bound MSs. The Leu_{MS} in the iridal vessels showed significantly higher values in iritis animals (IgG 5.1 ± 0.7, $n = 5$, $P = 0.004$, rPSGL-1 9.9 ± 1.2, $n = 8$, $P = 0.0001$) than in normal controls (IgG 0.4 ± 0.2, $n = 5$, rPSGL-1 0.6 ± 0.2, $n = 8$). Leu_{MS} in the iris vessels of iritis animals that were injected with rPSGL-1-conjugated MSs were significantly higher than in the mIgG-conjugated group ($P = 0.03$) (Figure 6C).

Molecular Imaging Evaluation of Anti-Inflammatory Treatment in the Iris

To investigate the potential of our molecular imaging approach in evaluation of anti-inflammatory interven-

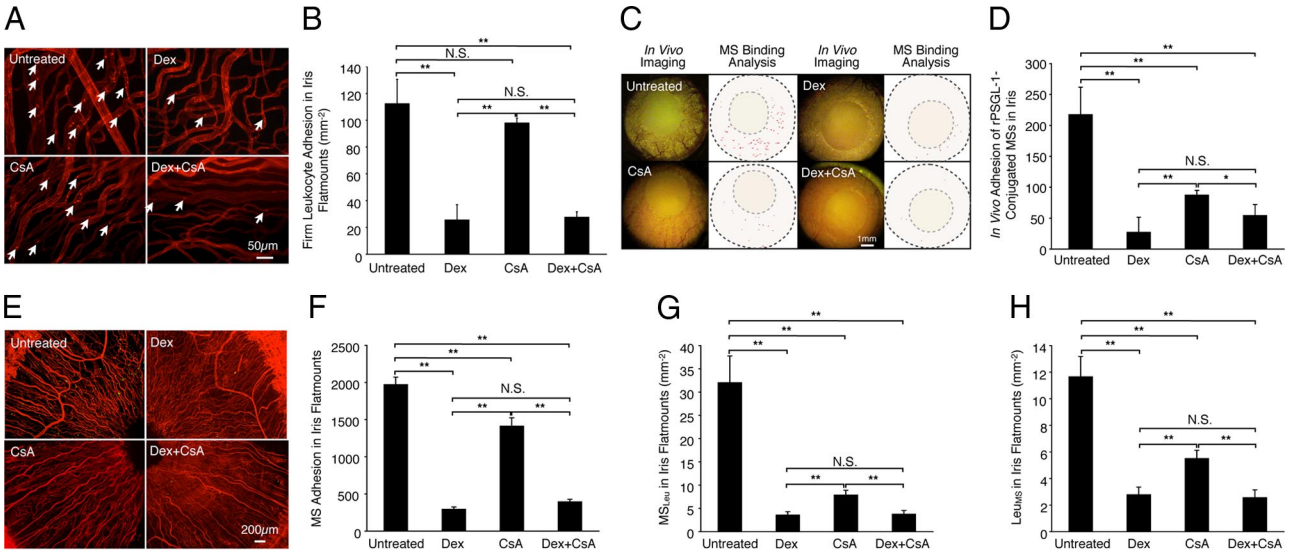

Figure 7. *In vivo* and *ex vivo* molecular evaluation of anti-inflammatory treatment success. Representative micrographs depicting iridal flat mounts of uveitic animals that were topically treated with eye drops of Dex or CsA. rPSGL-1-conjugated MSs were injected through the tail vein and 30 minutes later animals were perfused with rhodamine ConA to stain the vasculature and adherent leukocytes. **A:** *Ex vivo* visualization of firmly adhering leukocytes in the iridal microvasculature with or without Dex treatment. **Arrows** indicate firmly adhering leukocytes (bright red spots) inside the iridal microvessels. **B:** Quantitative comparison of the numbers of accumulated leukocytes in the iridal microvasculature per surface area (mm^{-2}), with or without topical anti-inflammatory treatments. $^{**}P < 0.01$; N.S., not significant. **C:** Video-micrographs of rPSGL-1-conjugated MS accumulation *in vivo* of uveitic animals with or without topical treatment, 30 minutes after MS injection. In the video still images (**left**), yellow-green spots delineate adhering MSs. In the ImageJ pictures (**right**), each dot indicates automated counts of adhering MSs in the iris vessels of normal and iritic animals. **D:** Quantitative comparison of *in vivo* MS accumulation in the total iridal vasculature of iritis animals using intravital microscopy, with or without topical anti-inflammatory treatments. $^{*}P < 0.05$; $^{**}P < 0.01$; N.S., not significant. **E:** *Ex vivo* visualization of accumulated MSs (yellow-green spots) in the iris flat mounts, with or without anti-inflammatory treatment. **F:** Quantitative comparison of *ex vivo* MS accumulation in total iridal flat mounts of iritis animals, with or without topical anti-inflammatory treatment. $^{**}P < 0.01$; N.S., not significant. **G:** The number of MSs binding to leukocytes (MS_{Leu}) in iridal microvasculature per surface area (mm^{-2}), with or without topical anti-inflammatory treatments. $^{**}P < 0.01$; N.S., not significant. **H:** The number of leukocytes binding to MSs (Leu_{MS}) in iridal microvasculature per surface area (mm^{-2}), with or without topical anti-inflammatory treatment. $^{**}P < 0.01$; N.S., not significant.

tions, we topically treated iritis animals with eye drops containing Dex, CsA, or both, and quantified the interaction of rPSGL-1-conjugated MSs with iridal vessels and leukocytes.

We compared the numbers of firmly adhering leukocytes in the surface area of the iris (per mm^2) in the eye drop–treated and untreated groups (Figure 7A). The adherent leukocyte numbers in the untreated animals (112.3 ± 18.3, $n = 6$) were significantly higher than in the three treated groups (Dex 25.6 ± 11.4, $n = 6$, $P = 0.008$, CsA 97.9 ± 3.6, $n = 6$, $P = 0.5$, Dex+CsA 27.6 ± 4.1, $n = 6$, $P = 0.006$), except for the leukocyte number in the CsA-treated group (Figure 7B).

In vivo fluorescent video microscopy showed significantly lower MS interaction in the topically treated groups (Dex 27 ± 7.5, $n = 6$, $P = 0.0003$; CsA 87.25 ± 17.8, $n = 6$, $P = 0.005$; Dex+CsA 54.25 ± 15.3, $n = 5$, $P = 0.001$) compared with the untreated iritis animals (217.3 ± 24.6, $n = 5$) (Figure 7, C and D). In iridal flat mounts, the number of accumulated MSs in the vessels of untreated iritis animals (1970 ± 101.7, $n = 5$) was significantly higher than Dex (338.6 ± 32.7, $n = 6$, $P = 1.5 \times 10^{-7}$), CsA (1411.8 ± 144.3, $n = 6$, $P = 0.01$), or doubly (Dex+CsA 393.8 ± 48.7, $n = 5$, $P = 6.1 \times 10^{-6}$) treated animals (Figure 7, E and F).

To investigate the impact of the topical anti-inflammatory drug treatments on the interaction of MSs with leukocytes in the iris vasculature, we calculated the number of MS_{Leu} and Leu_{MS} in the surface area of the iris (per mm^2) of the treated and untreated groups. MS_{Leu} in untreated animals (32.1 ± 5.7, $n = 6$) was significantly higher than in all three treated groups (Dex 3.6 ± 0.7, $n = 6$, $P = 0.0003$, CsA 7.9 ± 1, $n = 6$, $P = 0.009$, Dex+CsA 3.8 ± 0.8, $n = 6$, $P = 0.0001$) (Figure 7G). Similarly, Leu_{MS} was significantly higher in the untreated animals (untreated 11.6 ± 1.5, $n = 6$) than in the three treatment groups (Dex 2.8 ± 0.6, $n = 5$, $P = 2.5 \times 10^{-5}$, CsA 5.5 ± 0.6, $n = 6$, $P = 0.001$, Dex+CsA 2.6 ± 0.6, $n = 6$, $P = 6.7 \times 10^{-6}$) (Figure 7H).

Molecular Imaging Reveals Therapeutic Impact of Topical Anti-Inflammatory Eye Drops on Choroidal Vasculature

To evaluate whether the topical anti-inflammatory eye drops also affects other relevant vascular beds beyond the iridal microcirculation, we studied firm leukocyte adhesion and accumulation of our imaging agents in the retinal and choroidal microcirculation in LPS-injected animals. We compared the numbers of firmly adherent leukocytes in retinal flat mounts in the eye drop–treated and untreated groups (Figure 8, A and B). The adherent leukocyte numbers in the untreated animals (427.1 ± 32.8, $n = 6$) were significantly higher than in the three treated groups (Dex 298.3 ± 21.5, $n = 6$, $P = 0.007$, CsA 388.7 ± 67.7, $n = 6$, $P = 0.7$, Dex+CsA 267.6 ± 15.9, $n = 6$, $P = 0.005$), except for the leukocyte number in the CsA-treated group (Figure 8C). We compared the numbers of firmly adherent leukocytes in the surface area of the choroidal flat mount (per mm^2) in the eye drop treated and untreated groups (Figure 8D). The adherent leuko-

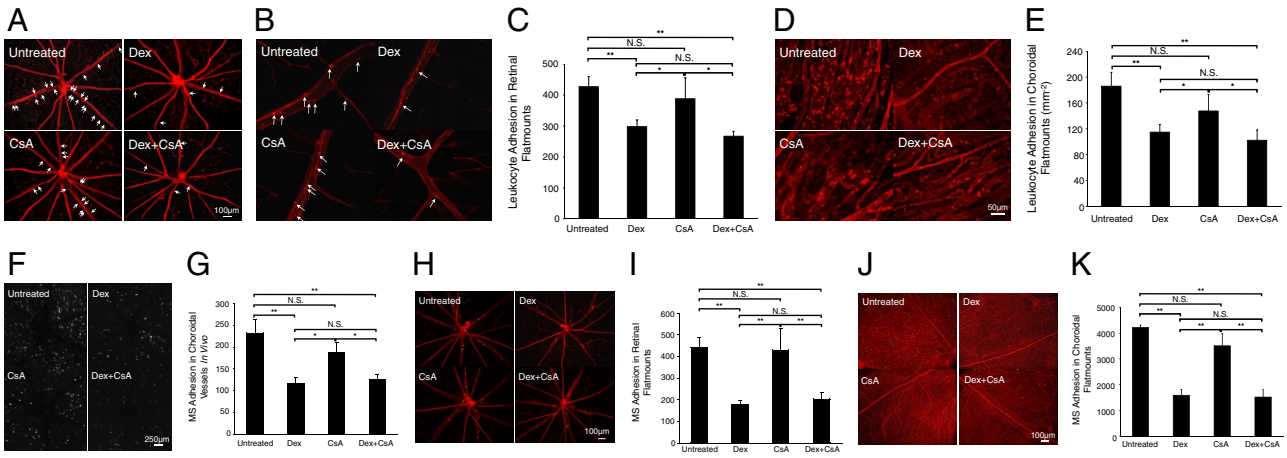

Figure 8. *In vivo* and *ex vivo* molecular evaluation of anti-inflammatory treatment success. Representative micrographs depicting SLO or flat mounts of retinal and choroidal vessels from uveitic animals that were topically treated with eye drops of Dex or CsA. rPSGL-1-conjugated MSs were injected through the tail vein and 30 minutes later animals were perfused with rhodamine ConA to stain the vasculature and adherent leukocytes. **A:** *Ex vivo* visualization of firmly adhering leukocytes (**arrows**) in the retinal flat-mount microvasculature of uveitic animals, with or without topical anti-inflammatory treatment. **B:** *Ex vivo* visualization of firmly adhering leukocytes in the retinal microvasculature of uveitic animals, with or without topical anti-inflammatory treatment. **Arrows**, firmly adhering leukocytes (bright red spots) inside the retinal microvessels. **C:** The number of firmly adhering leukocytes in retinal microvasculature of uveitic animals, with or without topical anti-inflammatory treatment. $^*P < 0.05$; $^{**}P < 0.01$; N.S., not significant. **D:** *Ex vivo* visualization of firmly adhering leukocytes in the choroidal flat-mount microvasculature of uveitic animals, with or without topical anti-inflammatory treatment. Bright red spots show firmly adhering leukocytes inside the choroidal microvessels. **E:** The number of firmly adhering leukocytes in choroidal microvasculature of uveitic animals, with or without topical anti-inflammatory treatment. $^*P < 0.05$; $^{**}P < 0.01$; N.S., not significant. **F:** *In vivo* SLO images of accumulated MSs in choroidal microvessels of uveitic animals, with or without topical anti-inflammatory treatments. White spots, firmly adhering MSs in the choriocapillaris. **G:** Quantitative comparison of *in vivo* MS accumulation in choroidal vessels of uveitic animals, with or without topical anti-inflammatory treatments using SLO. $^*P < 0.05$; $^{**}P < 0.01$; N.S., not significant. **H:** *Ex vivo* visualization of accumulated MSs (yellow-green spots) in the retinal flat mounts of uveitic animals with or without topical anti-inflammatory treatments. **I:** Quantitative comparison of *ex vivo* MS accumulation in total retinal flat mounts of LPS-injected animals, with or without topical anti-inflammatory treatments. $^{**}P < 0.01$; N.S., not significant. **J:** *Ex vivo* visualization of accumulated MSs (yellow-green spots) in the choroidal flat mounts of uveitic animals with or without topical anti-inflammatory treatments. **K:** Quantitative comparison of *ex vivo* MS accumulation in total choroidal flat mounts of LPS-injected animals, with or without topical anti-inflammatory treatments. $^{**}P < 0.01$; N.S., not significant.

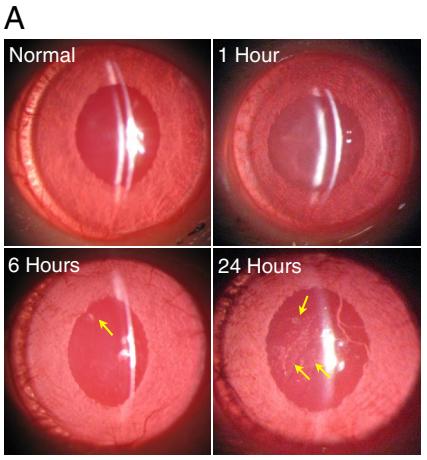

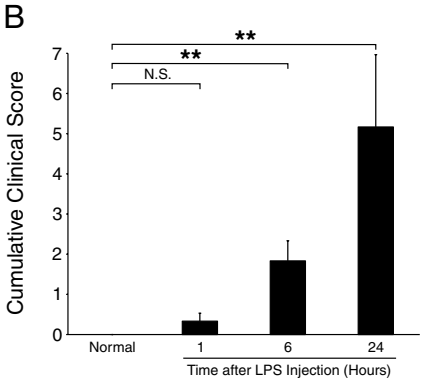

Figure 9. Imaging of slit-lamp examination in iris and AC. Anesthetized normal and iritic rats were clinically examined under slit-lamp. **A:** Normal animals show a clear AC without flare or effusion. LPS-injected animals show visible signs of inflammation in the AC, while the inflammatory reaction became progressively stronger with time. Twenty-four hours after LPS treatment, substantial effusions (**arrows**) and hypopyon were detected. **B:** Overall clinical score of normal were or LPS-treated rat eyes. $^{**}P < 0.01$; N.S., not significant.

cyte numbers in the untreated animals (186.3 ± 21.5, n = 6) were significantly higher than in the treated groups (Dex 114.9 ± 11.9, n = 6, P = 0.007, CsA 147.6 ± 25.3, n = 6, P = 0.3, Dex+CsA 102.3 ± 15.7, n = 6, P = 0.007), except for the leukocyte number in the CsA-treated group (Figure 8E).

In vivo SLO imaging of the choroidal microvasculature showed a significant decrease in the number of accumulated MSs in the Dex eye drop–treated and Dex+CsA-treated groups (Dex 116.4 ± 13.4, n = 5, P = 0.008; Dex+CsA 126 ± 10.5, n = 5, P = 0.01), compared with the untreated animals (232.6 ± 30.6, n = 5). However, in CsA-treated animals the number of MS accumulation did not differ significantly from the vehicle-treated controls (CsA 187.7 ± 23, n = 6, P = 0.2) (Figure 8, F and G).

In line with the *in vivo* results, retinal flat mounts of the Dex (178.3 ± 17.3, n = 5, P = 0.002) and Dex+CsA (202.4 ± 31.5, n = 5, P = 0.0006)-treated animals showed significantly lower numbers of MS adhesion than untreated animals (440.1 ± 43.5 n = 5), whereas topical CsA-treated animals did not show a significant difference compared with untreated animals (429.2 ± 100.5, n = 5, P = 0.7) (Figure 8, H and I).

The amount of MS adhesion in the choroidal flat mounts was comparable to that in the retinas. Untreated animals (4227.4 ± 91.2 n = 5) showed significantly higher adherent MS numbers than Dex (1588.5 ± 228.6, n = 5, P = 0.0001) or double-treated animals (1518.2 ± 287.3, n = 5, P = 0.0001), whereas CsA-treated animals (3512.3 ± 470.7, n = 5, P = 0.1) did not differ from untreated uveitic animals (Figure 8, J and K).

Subclinical Detection of Endothelial Injury: Comparison of MS Accumulation with the Existing Clinical and Experimental Evaluations

To find out whether our molecular imaging approach detects ocular inflammation earlier than the existing clinical or experimental techniques, we compared the time course (0, 1, 6, and 24 hours after LPS injection) of the cumulative clinical score of various readouts (flare, miosis, hypopyon, iris hyperemia, and leukocytes in the AC) and leukocyte recruitment with the imaging outcome of rPSGL-1-conjugated MS binding in iritic animals. AC examination showed cells in the aqueous humor, cloudiness of the light beam that was directed into the dark anterior chamber, as well as effusion, all of which progressed with the duration of the iritis (Figure 9A). The clinical score was significantly higher 6 hours (1.8 ± 0.5, n = 6 eyes, P = 0.003) and highest 24 hours (5.2 ± 1.7, n = 6 eyes, $P = 6 \times 10^{-6}$) after LPS injection, compared with normal animals (0 ± 0, n = 6). However, 1 hour after LPS injection (0.3 ± 0.2, n = 6, P = 0.14) the score did not differ from that of normal animals (Figure 9B).

In line with the cumulative clinical score, the numbers of the firmly adhering leukocytes in iridal flat mounts were significantly higher 6 hours (27.6 ± 8.4, n = 6, P = 0.02)

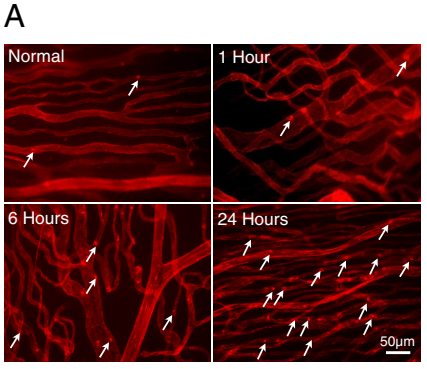

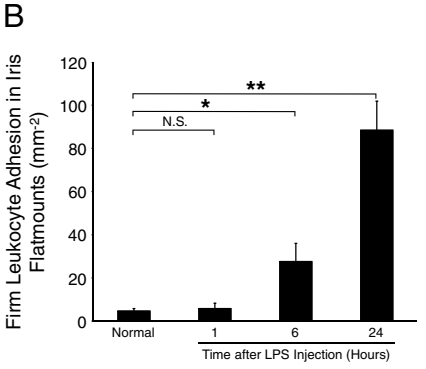

Figure 10. Time course of leukocytes accumulation in the iris vasculature. To quantify firm leukocyte adhesion, normal and LPS-injected animals were perfused with rhodamine ConA and iridal flat mounts were prepared. **A:** Representative micrographs indicate *ex vivo* visualization of firmly adhering leukocytes in the iridal microvasculature of normal or LPS-treated animals at different time points. **Arrows** indicate firmly adhering leukocytes (bright red spots) inside the iridal microvessels. **B:** Quantitative comparison of the numbers of accumulated leukocytes in iridal microvasculature per surface area (mm^{-2}), with or without LPS injection. $^{*}P < 0.05$; $^{**}P < 0.01$; N.S., not significant.

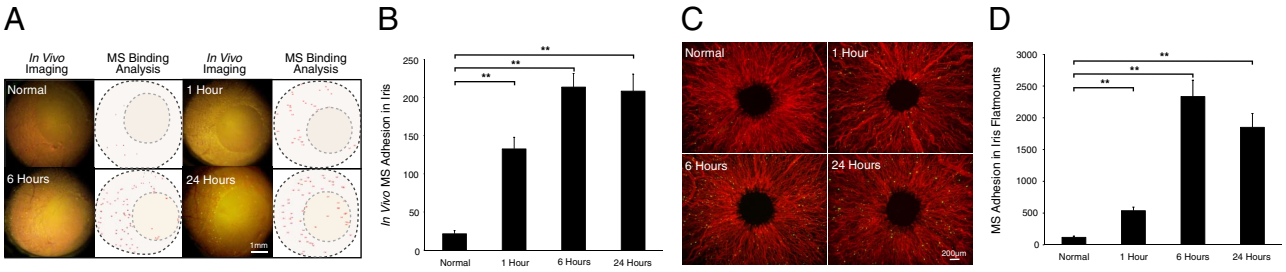

Figure 11. Subclinical detection of endothelial injury by noninvasive molecular imaging of iris. Intravital microscopy was performed and *ex vivo* flat mounts were generated at different time points after iritis induction to quantify the number of rPSGL-1-conjugated MSs in the iris vessels at different time points. **A:** Representative video micrographs of rPSGL-1-conjugated MS accumulation in normal and iritic animals, at the indicated time points after iritis induction and 30 minutes after MS injection. In the video still images, yellow-green spots delineate adhering MSs. In the ImageJ pictures, each dot indicates automated counts of adhering MSs in the iris vessels. **B:** Quantitative comparison of *in vivo* rPSGL-1-conjugated MS accumulation in the iridal vasculature of iritic animals. $^{**}P < 0.01$. **C:** *Ex vivo* visualization of accumulated MSs (yellow-green spots) in the iridal flat mounts of normal and iritic rats at the indicated time points. **D:** Quantitative comparison of *ex vivo* rPSGL-1-conjugated MS accumulation in iridal flat mounts of normal and iritic animals at the indicated time points. $^{**}P < 0.01$.

and highest at 24 hours after LPS injection (88.5 ± 13.4, $n = 6$, $P = 0.0002$), compared to normal animals (4.7 ± 1.1, $n = 6$). However, leukocyte accumulation did not differ from that in normal animals 1 hour after LPS injection (5.8 ± 2.5, $n = 6$, $P = 0.8$) (Figure 10, A and B).

In contrast to the cumulative clinical score and *ex vivo* leukocyte accumulation, *in vivo* molecular imaging with rPSGL-1-conjugated MSs showed a significantly higher binding (132.6 ± 15.3, $n = 6$, $P = 0.0003$) 1 hour after LPS injection, compared to the low amount of constitutive interaction in normal animals (21.4 ± 4.1, $n = 6$) (Figure 11, A and B). MS accumulation further increased by 6 hours (213.6 ± 17.9, $n = 6$, $P = 3.2 \times 10^{-5}$) and 24 hours (208.3 ± 22.4, $n = 6$, $P = 1.2 \times 10^{-4}$) after LPS injection. To confirm the *in vivo* findings, iridal flat mounts of ConA perfused animals were generated and the binding of the rPSGL-1-conjugated MSs quantitated *ex vivo*. Indeed, 1 hour after LPS injection there were significantly more MSs in the iris vessels (536.8 ± 57.6, $n = 6$, $P = 0.002$) than in the normal controls (117.3 ± 21.5, $n = 6$). The number of accumulated MSs further increased by 6 hours (2334.1 ± 258.5, $n = 6$, $P = 4.7 \times 10^{-4}$) and 24 hours (1849.4 ± 217.6, $n = 6$, $P = 0.0005$) after LPS injection (Figure 11, C and D).

Discussion

Noninvasive detection of molecular events in the living organism can revolutionize medicine. The eye provides a unique portal for visible light–based imaging of barrier-privileged and normal vessels. Under normal conditions, the AC is transparent. Extravasation of leukocytes or serum proteins into the AC under inflammatory conditions changes the optical properties of the aqueous humor, an observation, which is the mainstay of today's clinical evaluation. Before these cellular and structural changes occur, there are molecular manifestations of endothelial injury, knowledge of which would be of great scientific and clinical interest. The proximity of the well-perfused iris vasculature to the light-permeable cornea and its direct involvement in ocular inflammation make the iris an ideal target for noninvasive molecular imaging.

Using our previously introduced approach for endothelial surface molecule imaging,[9,10,13] we characterize endothelial injury in iritis animals *in vivo*. rPSGL-1-conjugated MSs accumulate significantly more in the iris vessels of uveitic animals, similar to the high number of accumulated leukocytes in iritis vessels. Strikingly, MS accumulation in the iris vasculature occurs earlier than the clinical signs of anterior uveitis or the increase in the number of firmly adhering leukocytes in the iris vasculature. This suggests that molecular imaging of iris vessels might truly reveal subclinical signs of the disease. Since the LPS-induced inflammation is primarily a systemic reaction, our approach carries the hope that in the future systemic diseases can be visualized through the eye.

Topical treatment with dexamethasone or CsA significantly reduces MS accumulation in the iris vessels, indicating suppression of endothelial adhesion molecule upregulation on treatment with these agents. The reduction of MS accumulation is larger than the reduction of leukocyte adhesion to the same vessels. This suggests that the anti-inflammatory treatment might be more effective in reducing the expression of individual adhesion molecules, while other adhesion molecules that provide a functional redundancy would suffice to uphold leukocyte adhesion.

Dexamethasone suppresses adhesion molecule expression in activated endothelium,[21] indicating that *in vivo* quantitation of adhesion molecule expression provides valuable insights about the degree of inflammation and therapeutic success. Surprisingly, topical anti-inflammatory treatment with dexamethasone makes a profound impact on MS accumulation in the fundus vasculature, similar to the effect it has on leukocyte recruitment, while CsA does not show an effect. Knowing which drugs can be used topically to cause beneficial effects in the fundus is clinically important, as the more convenient topical application of various drugs could replace their systemic application.

Beyond direct detection of endothelial injury, it is highly desirable to have quantitative knowledge of the number of accumulated immune cells in the ocular vessels. rPSGL-1-conjugated MSs bind to firmly adhering leukocytes, as leukocytes express L-selectin, the binding partner of PSGL-1. The significant interaction of rPSGL-1-conjugated MSs with firmly adhering leukocytes, as reflected in the Leu_{MS} and MS_{Leu} ratios, indicates that our

imaging probes reveal the amount of endogenous immune response in the iris vasculature. Confocal imaging shows that some of the MSs are indeed within leukocytes. This suggests that it might be possible to indirectly affect immune response by bringing MSs into the circulation that contains immunoregulatory drugs that are taken up by the leukocytes.

In summary, this work provides a novel means for quantitative assessment of endothelial injury in the iris vasculature. Molecular imaging of the iris presents a unique opportunity to visualize endothelial injury and immune response *in vivo*, due to the optical accessibility and involvement of the iris in ocular inflammatory diseases. Comparison of the vascular inflammatory response in the iris vessels with the choroidal or barrier-privileged retinal vessels provides valuable information about the impact of various drugs, depending on their route of application, and the evaluation of treatment success. Our imaging approach detects the earliest signs of disease, even before the occurrence of clinical symptoms, such as leakage, pain, or vision deterioration. On subclinical detection of molecular changes, effective treatments could be instituted to halt inflammation, before irreversible structural damage occurs. Besides being a powerful research tool, this versatile imaging approach has a high chance of being translated to the clinical realm and impacting the way medicine is practiced.

Acknowledgments

Research-grade YSPSL (Y's Therapeutics recombinant P-selectin glycoprotein ligand-1 Ig [rPSGL-Ig]) was a kind gift of Y's Therapeutics (San Bruno, CA). We thank Rebecca C. Garland for help in the preparation of this manuscript.

References

1. Rothova A, Suttorp-van Schulten MS, Frits Treffers W, Kijlstra A: Causes and frequency of blindness in patients with intraocular inflammatory disease. Br J Ophthalmol 1996, 80:332–336
2. Hafezi-Moghadam A, Noda K, Almulki L, Iliaki EF, Poulaki V, Thomas KL, Nakazawa T, Hisatomi T, Miller JW, Gragoudas ES: VLA-4 blockade suppresses endotoxin-induced uveitis: in vivo evidence for functional integrin up-regulation. FASEB J 2007, 21:464–474
3. Maruyama Y, Kishi S, Kamei Y, Shimizu R, Kimura Y: Infrared angiography of the anterior ocular segment, Surv Ophthalmol 1995, 39(Suppl 1):S40–S48
4. Rosenbaum JT, McDevitt HO, Guss RB, Egbert PR: Endotoxin-induced uveitis in rats as a model for human disease. Nature 1980, 286:611–613
5. Dullforce PA, Garman KL, Seitz GW, Fleischmann RJ, Crespo SM, Planck SR, Parker DC, Rosenbaum JT: APCs in the anterior uveal tract do not migrate to draining lymph nodes. J Immunol 2004, 172:6701–6708
6. Becker MD, Dullforce PA, Martin TM, Smith JR, Planck SR, Rosenbaum JT: Immune mechanisms in uveitis. What can be learned from in vivo imaging? Ophthalmol Clin North Am 2002, 15:259–270
7. Becker MD, Nobiling R, Planck SR, Rosenbaum JT: Digital video-imaging of leukocyte migration in the iris: intravital microscopy in a physiological model during the onset of endotoxin-induced uveitis. J Immunol Methods 2000, 240:23–37
8. Planck SR, Becker MD, Crespo S, Choi D, Galster K, Garman KL, Nobiling R, Rosenbaum JT: Characterizing extravascular neutrophil migration in vivo in the iris. Inflammation 2008, 31:105–111
9. Miyahara S, Almulki L, Noda K, Nakazawa T, Hisatomi T, Nakao S, Thomas KL, Schering A, Zandi S, Frimmel S, Tayyari F, Garland RC, Miller JW, Gragoudas ES, Masli S, Hafezi-Moghadam A: In vivo imaging of endothelial injury in choriocapillaris during endotoxin-induced uveitis. FASEB J 2008, 22:1973–1980
10. Sun D, Nakao S, Xie F, Zandi S, Schering A, Hafezi-Moghadam A: Superior sensitivity of novel molecular imaging probe: simultaneously targeting two types of endothelial injury markers. FASEB J 2010, 24:1532–1540
11. Parnaby-Price A, Stanford MR, Biggerstaff J, Howe L, Whiston RA, Marshall J, Wallace GR: Leukocyte trafficking in experimental autoimmune uveitis in vivo. J Leukoc Biol 1998, 64:434–440
12. Hafezi-Moghadam A, Ley K: Relevance of L-selectin shedding for leukocyte rolling in vivo. J Exp Med 1999, 189:939–948
13. Hafezi-Moghadam A, Thomas KL, Prorock AJ, Huo Y, Ley K: L-selectin shedding regulates leukocyte recruitment. J Exp Med 2001, 193:863–872
14. Laszik Z, Jansen PJ, Cummings RD, Tedder TF, McEver RP, Moore KL: P-selectin glycoprotein ligand-1 is broadly expressed in cells of myeloid, lymphoid, and dendritic lineage and in some nonhematopoietic cells. Blood 1996, 88:3010–3021
15. Spertini O, Cordey AS, Monai N, Giuffre L, Schapira M: P-selectin glycoprotein ligand 1 is a ligand for L-selectin on neutrophils, monocytes, and CD34+ hematopoietic progenitor cells. J Cell Biol 1996, 135:523–531
16. Moore KL: Structure and function of P-selectin glycoprotein ligand-1. Leukemia Lymphoma 1998, 29:1–15
17. Norman KE, Moore KL, McEver RP, Ley K: Leukocyte rolling in vivo is mediated by P-selectin glycoprotein ligand-1. Blood 1995, 86:4417–4421
18. Geng JG, Bevilacqua MP, Moore KL, McIntyre TM, Prescott SM, Kim JM, Bliss GA, Zimmerman GA, McEver RP: Rapid neutrophil adhesion to activated endothelium mediated by GMP-140. Nature 1990, 343:757–760
19. Abramoff MD, Magelhaes PJ, Ram SJ: Image processing with ImageJ. Biophotonics Int 2004, 11:36–42
20. Hoekzema R, Verhagen C, van Haren M, Kijlstra A: Endotoxin-induced uveitis in the rat. The significance of intraocular interleukin-6, Invest Ophthalmol Vis Sci 1992, 33:532–539
21. Cronstein BN, Kimmel SC, Levin RI, Martiniuk F, Weissmann G: A mechanism for the antiinflammatory effects of corticosteroids: the glucocorticoid receptor regulates leukocyte adhesion to endothelial cells and expression of endothelial-leukocyte adhesion molecule 1 and intercellular adhesion molecule 1, Proc Natl Acad Sci USA: 1992, 89:9991–9995